Image Quality and Activity Optimization in Oncologic F-18-FDG PET Using the Digital Biograph Vision PET/CT System

van Sluis, Joyce; Boellaard, Ronald; Dierckx, Rudi A; Stormezand, Gilles; Glaudemans, Andor W J M; Noordzij, Walter

Published in:
Journal of Nuclear Medicine

DOI:
10.2967/jnumed.119.234351

Publication date:
2020

Journal of Nuclear Medicine, published on October 18, 2019 as doi:10.2967/jnumed.119.234351

Image quality and activity optimization in oncological ^{18}F-FDG PET using the digital Biograph Vision PET/CT

Joyce van Sluis[1*], Ronald Boellaard[1], Rudi A.J.O. Dierckx[1], Gilles N. Stormezand[1], Andor W.J.M. Glaudemans[1], and Walter Noordzij[1]

*Correspondence: j.van.sluis@umcg.nl

ORCID ID: https://orcid.org/0000-0003-1908-4518

[1]Department of Nuclear Medicine and Molecular Imaging, University of Groningen, University Medical Center Groningen, Groningen, The Netherlands

Running title: Activity optimization with Vision PET/CT

Address for correspondence

Joyce van Sluis,

Department of Nuclear Medicine and Molecular Imaging

University Medical Center Groningen

Hanzeplein 1, 9713GZ, Groningen

The Netherlands

Word count: 4846

ABSTRACT

The first Siemens Biograph Vision PET/CT system (Siemens Healthineers, Knoxville, USA) was installed at the University Medical Center Groningen. Improved performance of this system could allow for a reduction in activity administration and/or scan duration. This study evaluates the effects of reduced scan duration in oncological ^{18}F-FDG PET imaging on quantitative and subjective imaging parameters and its influence on clinical image reading.

Methods: Patients referred for a clinical PET/CT scan were enrolled in this study, received a weight-based ^{18}F-FDG injected activity, and underwent a 180 seconds per bed position (s/bp) list-mode PET acquisition. Acquired PET data were reconstructed using the clinically vendor recommended reconstruction protocol (hereinafter referred to as Clinical), using the Clinical protocol with additional 2 mm Gaussian filtering (hereinafter referred to as Clinical+G2) as well as conform European Association of Nuclear Medicine Research Ltd (EARL) specifications using different scan durations per bed position (180, 120, 60, 30, and 10 s). Reconstructed images were quantitatively assessed for comparison of standardized uptake values (SUVs) and noise. In addition, Clinically reconstructed images were qualitatively evaluated by three nuclear medicine physicians.

Results: In total, 30 oncological patients (22 men, 8 women; age 48-88, mean ± SD 67 ± 9.6 years) received a single weight-based (3 MBq/kg) ^{18}F-FDG injected activity (weight 45-123 kg, mean ± SD 81 ± 15; activity 135-380 MBq, mean ± SD 241 ± 46.5). Significant differences in lesion SUVmax were found between the 180 s/bp images and the 30 and 10 s/bp images reconstructed using the Clinical protocols, whereas no differences were found in lesion SUVpeak. EARL compliant images did not show differences in lesion SUVmax or SUVpeak between scan durations. Quantitative parameters showed minimal deviation (~5%) in the 60 s/bp images. Further subjective image quality assessment was therefore conducted using the 60 s/bp images. Qualitative assessment revealed the influence of personal

preference on physicians' willingness to adopt the 60 s/bp images in clinical practice. Although quantitative PET parameters differed minimally, an increase in noise was observed.

Conclusions: Using the Biograph Vision PET/CT for oncological ^{18}F-FDG imaging, scan duration and/or activity administration could be reduced by a factor of three or more when using the Clinical+G2 or the EARL compliant reconstruction protocol, respectively.

Key words: Image quality, activity optimization, scan duration, SiPM, PET/CT

INTRODUCTION

Positron Emission Tomography (PET) integrated with Computed Tomography (CT) is a non-invasive imaging method widely used in oncology *(1–3)* and many other indications, providing both anatomic and metabolic information *(4)*. In oncology, PET/CT is a rapidly evolving technique for diagnosis, cancer staging, radiation therapy planning, prognosis, and treatment-response monitoring *(1,3,5)*.

Recently introduced PET/CT systems are equipped with silicon photomultiplier based detectors (SiPMs) with improved detection capabilities which may contribute to enhanced diagnostic performance, but could also allow for a reduction in activity administration and/or scan duration *(3,6–8)*. The first SiPM-based Siemens Biograph Vision PET/CT system (Siemens Molecular Imaging, Knoxville, USA) was installed at the department of Nuclear Medicine and Molecular Imaging at the University Medical Center Groningen in May 2018.

Despite of its frequent and widespread use in oncologic imaging, PET/CT is associated with some radiation exposure, particularly relevant for young lymphoma patients *(9)*. A pilot phantom study investigating the possibilities of activity reduction using the Biograph Vision PET/CT (Supplemental section *(6)* showed 2-deoxy-2-[fluorine-18] fluoro-D-glucose (^{18}F-FDG) administration can be decreased by a factor of approx. eight for scanning 60 seconds per bed position (s/bp) using European Association of Nuclear Medicine (EANM) Research Ltd. (EARL) compliant reconstructions *(1,10)*. Lowering the injected activity results in a decrease in radiation exposure for young patients as well as medical staff, but can also reduce ^{18}F-FDG costs. On the other hand, shorter scan times can increase patient throughput which in turn increases cost-effectiveness.

To our knowledge, scan duration and/or activity optimization has not yet been explored for the Biograph Vision PET/CT. Therefore, to further clinically validate the findings obtained from our phantom measurements, the effects of scan duration and/or administered activity reduction in ^{18}F-FDG PET

imaging on quantitative and subjective imaging parameters and its influence on clinical image reading was evaluated in this study.

MATERIALS AND METHODS

Patient Population

Patients referred for an oncological clinical PET/CT were enrolled in this prospective study. For optimal comparison of quantitative parameters, three different malignancies were selected to form homogeneous groups: non-small cell lung carcinoma (NSCLC), esophageal cancer, and lymphoma. Patients with a glucose level $\geq$ 198 mg/dL prior to ^{18}F-FDG administration were excluded from participation in this study.

According to the Dutch Medical Research Involving Human Subject Act, the local medical ethical committee exempted approval without additional procedures (waiver number: METc2017/489). No additional informed consent was required. Patient information was anonymized before data analysis.

Imaging Protocol

According to EANM guidelines for tumor imaging, patients received a weight-based bolus injection of ^{18}F-FDG activity (3 MBq/kg) via intravenous infusion *(1,11)*. The syringe and catheter were not measured after the injection for any residual activity. Approximately 60 min post injection (mean ± SD 62 ± 5), patients underwent a list-mode PET/CT imaging protocol on the Biograph Vision system.

Patients were instructed to avoid strenuous exercise for 24 hours and to fast for at least 4-6 hours prior to ^{18}F-FDG activity administration. At the time of ^{18}F-FDG injection, blood glucose levels measured $\leq$ 198 mg/dL. A standard low dose CT (an X-ray tube current of 43 mAs, a tube voltage of 100 kV, and a spiral pitch factor of 1) was acquired from the vertex to the mid-thigh and used for attenuation correction. A consecutive emission PET scan was acquired in 180 s/bp in list-mode. All scans were obtained during normal breathing.

Subsequently, PET list mode data was reprocessed to produce additional sets of sinograms: 10, 30, 60, and 120 s/bp. Three different reconstruction protocols were used to reconstruct the PET images

for each of the five scan durations. The clinically vendor recommended reconstruction protocol, i.e., an ordinary Poisson ordered-subset expectation maximization (OP-OSEM) 3D-iterative algorithm *(12)* using 4 iterations, 5 subsets, Time-of-Flight application, resolution modeling, without filtering (hereinafter referred to as Clinical) and with 2 mm Gaussian filtering (hereinafter referred to as Clinical+G2). The resulting image size was 440x440 with a voxel size of 1.6x1.6x1.5 mm. In addition, the EARL1 and EARL2 reconstructions *(1,10)* were obtained using 3D OP-OSEM, Time-of-Flight application, with 4 iterations and 5 subsets, with application of resolution modelling and a Gaussian filter of 7 mm and 5 mm, respectively. The resulting image size was 220x220 with a voxel size of 3.3x3.3x1.5 mm.

All scans were acquired during normal breathing without respiratory motion gating or correction.

Quantitative Image Analysis

Reconstructed PET images were analyzed using the quAntitative onCology moleCUlar Analysis suiTE (ACCURATE) version v03012019 *(13)*. Two semi-automated tumor delineation methods were used to segment and analyze individual lesions per image (with a maximum of the 10 hottest lesions). The first semi-automated method is based on a fixed standardized uptake value (SUV) threshold of 4.0 g/mL (SUV = 4), whereas the other method, so-called Majority Vote (MV2), is based on agreement in tumor delineation between multiple semi-automated methods *(14)*. For clarity, an illustrative clinical image example and a schematic overview of the MV2 method is shown in supplemental Figures 1 and 2, respectively. In case the semi-automated methods were incapable of delineating the lesion, a 1 mL spherical volume of interest (VOI) was manually placed on (the hottest part in) the lesion. Analyses were performed using SUVmax and SUVpeak measurements (derived from semi-automated delineation or the manual VOI placement), obtained from the 2 successfully applied semi-automated delineation methods.

In addition, for each image a 3 mL spherical VOI was placed in the liver, where activity is distributed almost uniform, as a reference and to characterize the image noise using the standard deviation of the voxel values within the VOI.

Qualitative Image Analysis

Images obtained at 180 s/bp and at shorter scan duration (i.e. 60 s/bp) using the Clinical reconstruction protocols were qualitatively evaluated. The 60 s/bp data were chosen because for this shorter duration the images were quantitatively still comparable with those at 180 s/bp (as will be shown later). Three experienced nuclear medicine physicians (AG, GS, and WN: 15, 5, and 10 years of experience in interpreting PET scans, respectively) independently reviewed the reconstructed images using a dedicated *syngo*.via VB30 (Siemens Healthineers) workstation. Readers were not blinded for scan duration. Images reconstructed according to the Clinical protocol were evaluated first. After four weeks, images reconstructed according to the Clinical+G2 were evaluated. Images were scored based on 5-point Likert scales with regard to the following characteristics: image noise, lesion margin demarcation, and overall image quality. In addition, the number of avid ^{18}F-FDG lesions per image was counted to assess possible missed lesions in shorter scan durations and TNM staging was performed.

Statistical Analysis

Analyses were performed with SPSS Statistics, version 25.0 (IBM Corp., Armonk, NY). Per reconstruction method, lesion SUVs at each scan duration, 120, 60, 30, and 10 s/bp, were compared to the lesion SUVs of images acquired at 180 s/bp using a repeated measures analysis of variance (ANOVA) with post hoc Bonferroni adjustment for pairwise comparison. A *P* value of less than 0.05 was considered significant. Pairwise comparisons were also performed to assess the differences between each lesion's SUVmax derived from the 180 s/bp images and shorter scan durations.

All quantitative analyses were performed in two-fold; once for the quantitative parameters obtained using the SUV = 4 semi-automated delineation method and once for the parameters obtained using the MV2 semi-automated delineation method.

Furthermore, qualitative Likert-scale scores of the images were compared pairwise using a two-tailed paired samples t-test, in addition inter-reader agreement was evaluated using kappa statistics.

RESULTS

A total of 30 oncological patients (22 men, 8 women; age 48-88, mean ± SD 67 ± 9.6 years) received a single weight-based bolus of ^{18}F-FDG injected activity (weight 45-123 kg, mean ± SD 81 ± 15; activity 135-380 MBq, mean ± SD 241 ± 46.5) via intravenous infusion. For optimal quantitative comparison, three homogeneous groups were formed consisting of 15 NSCLC patients, 9 patients with lymphoma, and the remaining 6 were diagnosed with esophageal cancer. Table 1 shows relevant demographic and clinical information.

Quantitative Image Analysis

For each of the 30 patients, a total of 20 images were obtained (four reconstruction methods times five scan durations times 30 patients results in 600 images). Tumor segmentations were performed on each of the 600 images individually. In total, 4076 tumor segmentations were made; a total of ∼100 tumor lesions were segmented using 2 semi-automated segmentation methods (SUV = 4 and MV2) for each reconstructed scan duration and each reconstruction method, resulting in 40 segmentations per lesion. 352 lesion segmentations could not be made by the SUV = 4 method, whereas the MV2 method was unsuccessful in capturing 1155 lesion segmentations. Median lesion SUVmax was 8.7 (range 1.7 – 57) and median lesion SUVpeak was 3.9 (range 0.2 – 59).

Results of the lesion SUVmax comparisons between different scan durations obtained using the SUV = 4 and the MV2 semi-automated lesion delineation methods for the three different reconstruction protocols are shown in boxplots in Figure 1. Similarly, the results of the lesion SUVpeak comparisons are shown in Figure 2. Differences in SUVmax comparisons per lesion between measurements derived from the 180 s/bp images and measurements done at shorter scan durations for the four different reconstruction protocols, delineated using both semi-automated methods, are illustrated in boxplots in Figure 3.

For additional clarification, differences in median lesion SUVmax obtained at shorter scan durations directly compared to the 180 s/bp derived values, delineated by both semi-automated methods are summarized in Table 2.

Using the Clinical and Clinical+G2 reconstruction settings, a significant difference in lesion SUVmax was found between the 180 s/bp and the 10 s/bp images when delineated with the SUV = 4 method, ($P < 0.01$, 95% Confidence interval (CI) (0.50 – 5.91) and $P < 0.001$, 95% CI (0.85 – 3.65)). In addition, using the Clinical+G2 reconstruction settings, a significant difference in lesion SUVmax was found between the 60 s/bp and the 10 s/bp images ($P < 0.05$, 95% CI (0.24 – 3.42)).

When delineations were performed with the MV2 method, a significant difference in lesion SUVmax in the Clinically reconstructed images between the 180 s/bp and both the 30 and 10 s/bp images was found ($P < 0.05$, 95% CI (0.12 – 4.10) and $P < 0.001$, 95% CI (0.99 – 5.85), respectively). A significant difference was also found between the 120 s/bp and both the 30 and 10 s/bp images ($P <$ 0.05, 95% CI (0.30 – 3.38) and 95% CI (0.47 – 5.83), respectively). As well as between the 60 s/bp images and 30 s/bp images ($P < 0.001$, 95% CI (0.43 – 2.09)). Between the images obtained using the Clinical+G2 reconstruction method, a significant difference in lesion SUVmax between the 180 s/bp and the 10 s/bp was found ($P < 0.05$, 95% CI (0.02 – 0.28)) as well as between the 120 s/bp and 10 s/bp ($P < 0.05$, 95% CI (0.31 – 3.85), and between the 60 s/bp and both the 30 and 10 s/bp images ($P < 0.001$, 95% CI (0.39 – 1.05) and $P < 0.05$ 95% CI (0.21 – 4.20), respectively).

No significant differences were found between lesion SUVpeak at different scan durations. Furthermore, EARL1 and EARL2 reconstructed images did not show any significant differences in SUVmax or SUVpeak compared between all different scan durations.

Qualitative Image Analysis

From the quantitative analysis, the shorter scan duration still quantitatively resembling the values obtained from the 180 s/bp images reconstructed according to the Clinical and Clinical+G2 protocol (deviation of ~5%) was found to be the 60 s/bp option (see Fig. 1 and Table 2). Further clinical evaluations were therefore conducted with the 180 s/bp images and the 60 s/bp images. For illustrative purposes, Figure 4 shows example patient PET images acquired using the four reconstruction protocols at different scan durations ranging from 180 s/bp to 10 s/bp. Figures 5 and 6 show reconstructed example patient PET images obtained using the four different reconstruction settings at 180 s/bp directly compared to 60 s/bp.

All 180 s/bp images reconstructed using the Clinical reconstruction protocol were scored significantly higher than the images acquired at 60 s/bp on noise, lesion demarcation and overall image quality ($P < 0.001$, 95% CI (2.25 – 2.55), 95% CI (2.03 – 2.35), and 95% CI (2.20 – 2.58), respectively). Using the Clinical+G2 protocol, images obtained at 180 s/bp were scored higher than the 60 s/bp images as well. In addition, the filtered images were more highly valued with respect to their unfiltered counterparts ($P < 0.001$, 95% CI (2.87 – 3.20), 95% CI (3.02 – 3.24), and 95% CI (3.16 – 3.35), respectively). In case of the images reconstructed according to the Clinical protocol, Fleiss kappa did not show significant inter-reader agreement. For the Clinically reconstructed images with additional 2 mm filtering, inter-reader agreement was good regarding evaluation of noise, lesion demarcation and overall image quality with a kappa of 0.65 ($P < 0.001$, 95% CI (0.57 – 0.74)), 0.64 ($P < 0.001$, 95% CI (0.56 – 0.73)), and 0.72 ($P < 0.001$, 95% CI (0.64 – 0.81)), respectively.

With regard to the images reconstructed according to the Clinical protocol, in 5 out of 30 cases, reducing scan duration from 180 s/bp to 60 s/bp resulted in missed lesions changing the TNM staging of the disease. In 2 of these cases, the change in TNM staging would have influenced the choice of therapy. In these two cases, two NSCLC patients, the missed lesions were specifically a contralateral lung nodule in one patient and a distant liver metastasis in the other. There was no inter-reader agreement on

exchanging 180s/bp images for the shorter acquisition time, since the reading physicians were willing to exchange the 180 s/bp for the 60s/bp images in 27, 8, and 23 cases, respectively.

Concerning the images reconstructed using the Clinical+G2 protocol, in 1 out of 30 cases, reducing scan duration from 180 s/bp to 60 s/bp resulted in a missed lesion changing the TNM staging of the disease. This missed lesion would not have had any influence on the therapy choice for this patient as it was one of three small locoregional lymph node metastases from a primary esophageal carcinoma. There was no inter-reader agreement on exchanging 180 s/bp images for the shorter acquisition time, since the reading physicians were willing to exchange the 180 s/bp for the 60 s/bp images in 13, 24, and 21 cases, respectively.

Results of the noise quantification through calculation of the coefficient of variance (COV) obtained from the 3 mL liver VOIs in each image are shown in Figure 7. Here, a difference in the amount of image noise can be observed between images obtained at 180 s/bp and images obtained at 60 s/bp for all four reconstruction protocols.

DISCUSSION

In this study, the effect of scan time reduction on quantitative PET image parameters and image quality using the digital Biograph Vision PET/CT system has been explored. Administered ^{18}F-FDG activity can be adjusted proportionally to shorter scan times per bed position (with an added 10% for compensation of lower noise equivalent count rates per MBq at higher activity concentrations) *(5)*. The results using the Clinical protocols suggest that with a minimal bias (approx. 5%) on quantitative image parameters, it is feasible to reduce scan time or activity by a factor of three when using the Clinical and Clinical+G2 reconstruction protocol. When applying EARL compliant reconstructions, even further reductions are potentially achievable *(6)*.

Image quality of PET images obtained at reduced scan duration was evaluated by three nuclear medicine physicians to assess its impact in clinical practice. From this evaluation it became apparent that personal preference is an essential element contributing to physicians' willingness to adopt the shorter scan duration for diagnosing in clinical practice. Although quantitative PET parameters differed minimally, a substantial increase in noise was observed (see Fig. 7). The extent to which this increase in noise is disturbing to the physician, is decisive for the scoring of image quality and for the consideration of working with the shorter scan duration. The addition of a small Gaussian filter of 2 mm to the reconstruction protocol in the 60 s/bp setting diminished the influence of image noise, without notably affecting the apparent spatial resolution *(15)*.

Using the Clinical+G2 reconstruction protocol, reduction of scan time and/or injected activity could lead to downstaging in only 1 out of 30 cases as indicated by two out of three nuclear medicine specialists. The three nuclear medicine physicians evaluated the shorter scan duration images as they would have done with the 180 s/bp. When taking some extra time, possibly this now missed lesion would not have been overlooked in the 60 s/bp images. A trade-off between increasing patient through

put and/or reducing radiation exposure and possibly reserving more time for image reading is a factor that needs to be taken into consideration.

With regard to other commercially available digital PET/CT systems, a comparable study stated that a reduction in activity or scan time to 90 s/bp (which equals a factor of two) is feasible when using the Discovery MI PET/CT (GE Healthcare) *(16)*. For the Vereos PET/CT system (Philips Healthcare) a similar study on activity optimization has not been conducted yet.

This is the first study to explore scan duration and/or activity optimization and image quality using the digital Biograph Vision PET/CT system. Lowering the injected activity by a factor of three will result in a decrease in radiation exposure for patients (particularly important in case of young lymphoma patients) as well as medical staff, and will also reduce ^{18}F-FDG costs, while maintaining quantitative PET performance. For institutions more interested in increased patient throughput, shorter scan times (down to approx. 6 min for a whole-body scan) in combination with an activity prescription of 3 MBq/kg are feasible using the Biograph Vision, which in turn also increases cost-effectiveness. However, with increasing patient throughput, there is also more demand for peripheral sources such as preparation rooms, staff, time for reporting, etc. For pediatric purposes, both reducing activity and faster scanning is of high clinical importance as radiation exposure should be kept to the bare-minimum in this patient population, whereas faster scanning decreases the need for anesthetics.

CONCLUSION

When using the Biograph Vision PET/CT for oncological ^{18}F-FDG imaging, it is acceptable for routine clinical imaging to reduce scan duration or activity administration by a factor of three compared to EANM activity prescriptions *(1)* when using the Clinical+G2 reconstruction protocol. When applying EARL compliant reconstructions, further reductions are achievable, depending on local preferences.

A reduction in injected activity decreases radiation exposure for patients as well as for medical staff. In addition, for institutions without the ability to produce their own ^{18}F-FDG, activity reduction will lower the costs of PET/CT imaging. Alternatively, a faster scan time increases patient throughput resulting in a higher cost efficiency for PET centers.

ACKNOWLEDGEMENTS

The research presented in this study is financially supported by Siemens Molecular Imaging under a collaborative research contract. No other potential conflict of interest relevant to this article was reported.

KEY POINTS

QUESTION: Does the new Siemens Biograph Vision PET/CT allow for a reduction in scan duration and/or activity administration to decrease radiation exposure and/or reduce ^{18}F-FDG PET imaging costs?

PERTINENT FINDINGS: Images of 180 s/bp were quantitatively compared to images acquired at shorter scan durations in 30 patients referred for an oncological clinical PET/CT. The optimal shorter scan duration, still quantitatively representative for the 180 s/bp images (with approx. 5% bias), was found to be 60 s/bp. The extent to which three nuclear medicine physicians regarded the increase in noise in the 60 s/bp images as disturbing was decisive for their willingness to adopt the shorter scan duration for diagnosing in clinical practice.

IMPLICATIONS FOR PATIENT CARE: Using the Biograph Vision, administered ^{18}F-FDG activity or scan duration can be reduced by a factor of three which decreases patients' radiation exposure or increases patient throughput.

REFERENCES

1. Boellaard R, Delgado-Bolton R, Oyen WJG, et al. FDG PET/CT: EANM procedure guidelines for tumour imaging: version 2.0. Eur J Nucl Med Mol Imaging. 2014;42:328–54.
2. Slomka PJ, Pan T, Germano G. Recent advances and future progress in PET instrumentation. Semin Nucl Med. 2016;46:5–19.
3. Hsu DFC, Ilan E, Peterson WT, Uribe J, Lubberink M, Levin CS. Studies of a next-generation silicon-photomultiplier–based time-of-flight PET/CT system. J Nucl Med. 2017;58:1511–8.
4. Townsend DW. Dual-modality imaging: combining anatomy and function. J Nucl Med. 2008;49:938–55.
5. Boellaard R, Oyen WJG, Hoekstra CJ, et al. The Netherlands protocol for standardisation and quantification of FDG whole body PET studies in multi-centre trials. Eur J Nucl Med Mol Imaging. 2008;35:2320–33.
6. Sluis J Van, Jong J De, Schaar J, et al. Performance characteristics of the digital Biograph Vision PET/CT system. J Nucl Med. 2019;60:1031–1036.
7. Nguyen NC, Vercher-Conejero JL, Sattar A, et al. Image quality and diagnostic performance of a digital PET prototype in patients with oncologic diseases: initial experience and comparison with analog PET. J Nucl Med. 2015;56:1378–85.
8. Rausch I, Ruiz A, Valverde-Pascual I, Cal-González J, Beyer T, Carrio I. Performance evaluation of the Philips Vereos PET/CT System according to the NEMA NU2-2012 standard. J Nucl Med. 2018;60:561–7.
9. Karakatsanis NA, Fokou E, Tsoumpas C. Dosage optimization in positron emission tomography: state-of-the-art methods and future prospects. Am J Nucl Med Mol Imaging. 2015;5:527–47.
10. Boellaard R. New developments of EANM oncology PET/CT guidelines and update of the EARL accreditation standards presentation. 2018. Available from: http://earl.eanm.org/html/img/pool/New_EARL_project_and_update_of_FDG_standard_Oct2018.pdf. Accessed May 7, 2019.
11. Boellaard R, Doherty MJO, Weber WA, et al. FDG PET and PET/CT: EANM procedure guidelines for tumour PET imaging: version 1.0. Eur J Nucl Med Mol Imaging. 2010;37:181–200.
12. Varrone A, Sjöholm N, Eriksson L, Gulyás B, Halldin C, Farde L. Advancement in PET quantification using 3D-OP-OSEM point spread function reconstruction with the HRRT. Eur J Nucl Med Mol Imaging. 2009;36:1639–50.
13. Boellaard R. Quantitative oncology molecular analysis suite: ACCURATE. J Nucl Med. 2018 May 1;59(supplement 1):1753–1753.
14. Kolinger GD, Vállez García D, Kramer GM, et al. Repeatability of [18 F]FDG PET/CT total metabolic active tumour volume and total tumour burden in NSCLC patients. EJNMMI Res. 2019;9:14.
15. Armstrong IS, Kelly MD, Williams HA, Matthews JC. Impact of point spread function modelling and time-of-flight on FDG uptake measurements in lung lesions using alternative filtering strategies. EJNMMI Phys. 2014;1:99.
16. Sonni I, Baratto L, Park S, et al. Initial experience with a SiPM-based PET/CT scanner: influence

of acquisition time on image quality. EJNMMI Phys. 2018;5:9.

Table 1 – Demographic and clinical data of all included patients.

Patient #	Age (y)	Sex	Weight (kg)	Disease	Injected ^{18}F-FDG activity (MBq)
1	74	M	75	NSCLC	215
2	74	M	87	NSCLC	270
3	70	M	66	NSCLC	195
4	65	M	87	NSCLC	265
5	61	M	77	NSCLC	231
6	62	M	91	NSCLC	275
7	59	F	70	NSCLC	220
8	67	F	85	NSCLC	260
9	79	M	90	NSCLC	265
10	63	M	76	NSCLC	205
11	61	F	87	NSCLC	260
12	53	F	45	NSCLC	135
13	81	M	58	NSCLC	160
14	88	M	88	NSCLC	264
15	69	F	76	NSCLC	220
16	77	F	71	Lymphoma	210
17	48	M	82	Lymphoma	240
18	75	M	80	Lymphoma	245
19	61	M	90	Lymphoma	280
20	62	F	68	Lymphoma	220
21	62	M	88	Lymphoma	260
22	72	M	86	Lymphoma	270
23	70	F	58	Lymphoma	180
24	64	M	90	Lymphoma	280
25	60	M	106	Esophageal cancer	305
26	77	M	62	Esophageal cancer	200
27	58	M	123	Esophageal cancer	380
28	84	M	73	Esophageal cancer	220
29	70	M	101	Esophageal cancer	290
30	52	M	86	Esophageal cancer	260

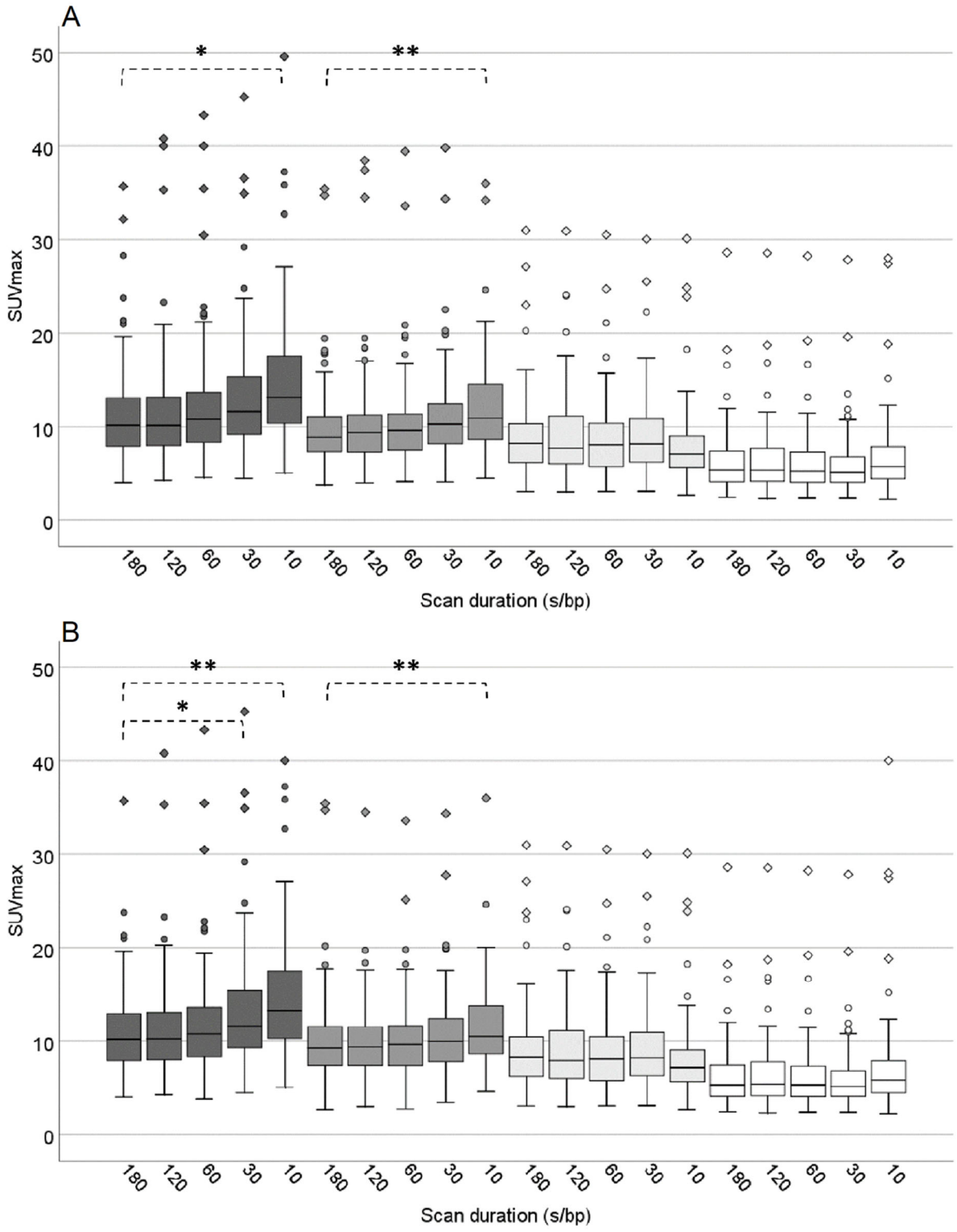

Figure 1 – Boxplots showing the spread of SUVmax obtained from the Clinical (dark grey), Clinical+G2 (grey), EARL2 compliant (light grey), and EARL1 compliant (white) reconstructed images at different scan durations. Quantitative analyses were performed using the SUV = 4 (A) and the MV2 (B) semi-automated lesion delineation method. Outliers are illustrated with dots,

the diamonds represent extreme outliers. * and ** indicate a significant difference of $P < 0.05$ and $P < 0.001$ between scan durations, respectively.

Table 2 – Median lesion SUVmax scores derived from images obtained using the Clinical and Clinical+G2 reconstruction settings, delineated with both the SUV = 4 and MV2 semi-automated delineation method. Bias is the percentage difference between median SUVmax at shorter scan durations and the median SUVmax of the 180 s/bp images.

	SUV = 4		MV2	
Scan duration (s/bp)	**Median SUVmax**	**Bias (%)**	**Median SUVmax**	**Bias (%)**
CLINICAL				
180	10.39	n.a.	10.27	n.a.
120	10.43	0.4	10.28	0.1
60	10.99	5.8	10.83	5.5
30	11.79	13.5	11.63	13.3
10	13.14	26.5	13.20	28.6
CLINICAL+G2				
180	9.33	n.a.	9.44	n.a.
120	9.71	4.2	9.61	1.9
60	10.02	7.4	9.88	4.7
30	10.61	13.7	10.33	9.5
10	11.67	25.2	11.30	19.8

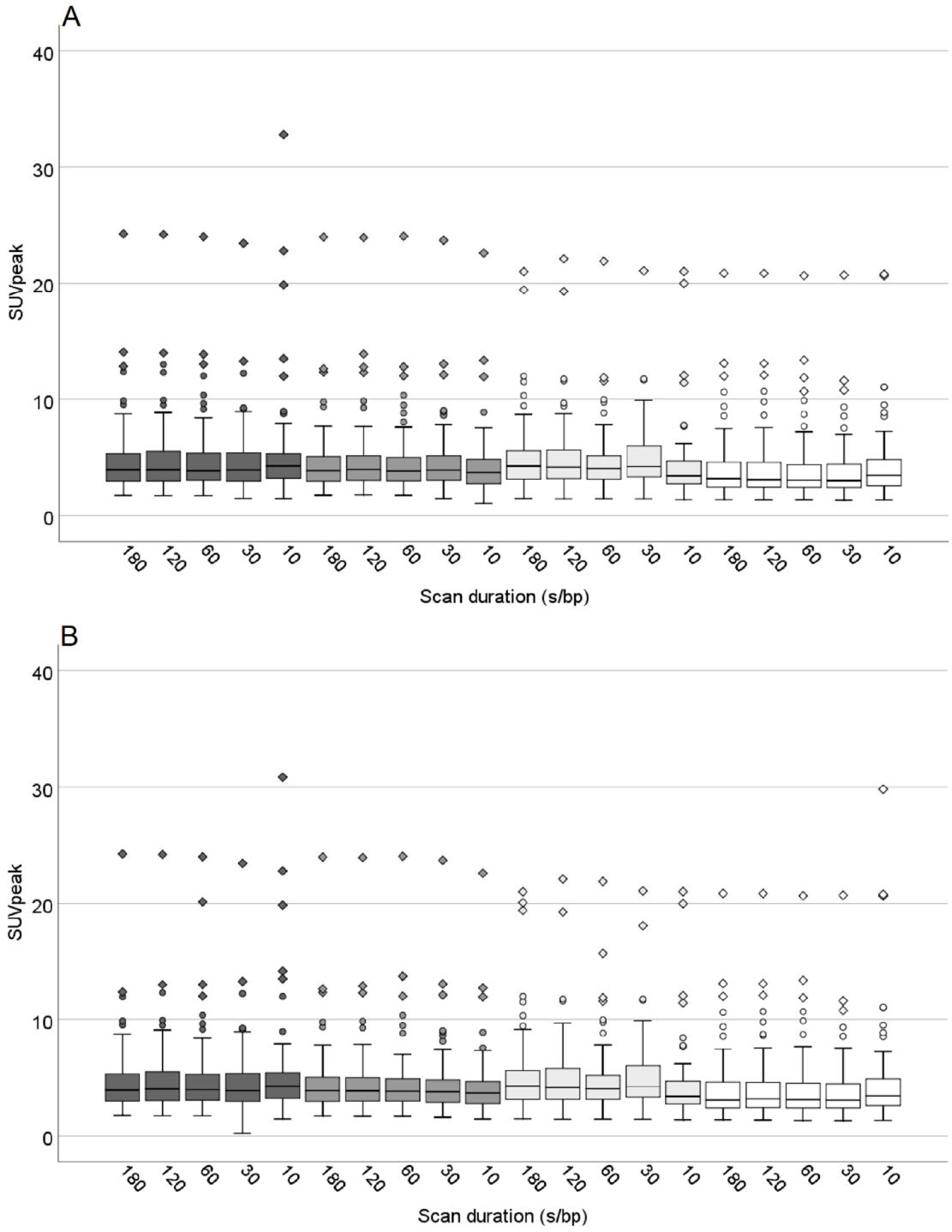

Figure 2 – Boxplots showing the spread of SUVpeak obtained from the Clinical (dark grey), Clinical+G2 (grey), EARL2 compliant (light-grey), and EARL1 compliant (white) reconstructed images at different scan durations. Quantitative analyses were performed using the SUV = 4 (A) and the MV2 (B) semi-automated lesion delineation method. Outliers are illustrated with dots, the diamonds represent extreme outliers.

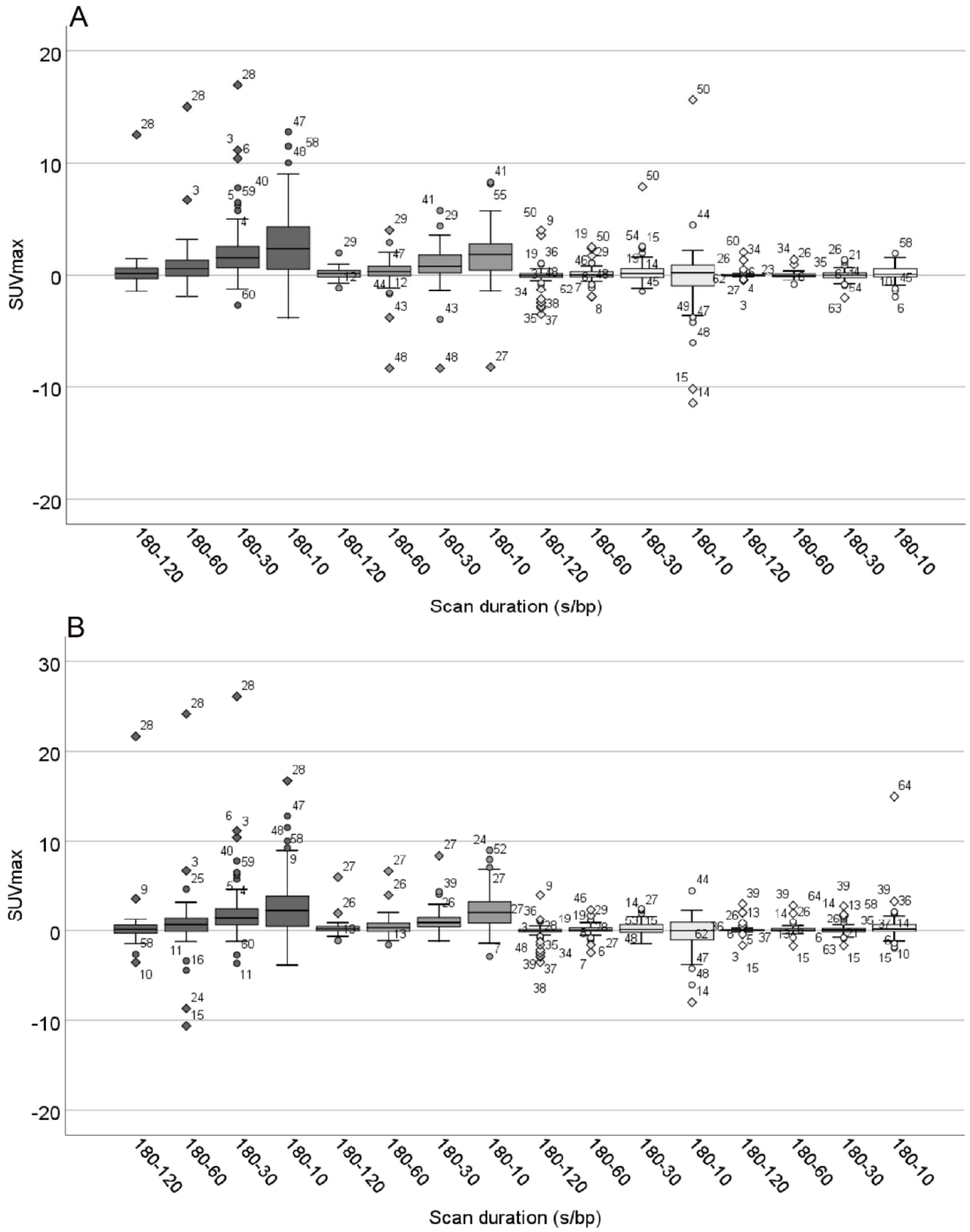

Figure 3 – Boxplots showing the spread of SUVmax differences per lesion between the 180 s/bp and shorter scan durations obtained from the Clinical (dark grey), Clinical+G2 (grey), EARL2 compliant (light grey), and EARL1 compliant (white) reconstructed images. Quantitative analyses were performed using the SUV = 4 (A) and MV2 (B) semi-automated lesion delineation method. Outliers are illustrated with dots, the diamonds represent extreme outliers, the numbers indicate the lesion number.

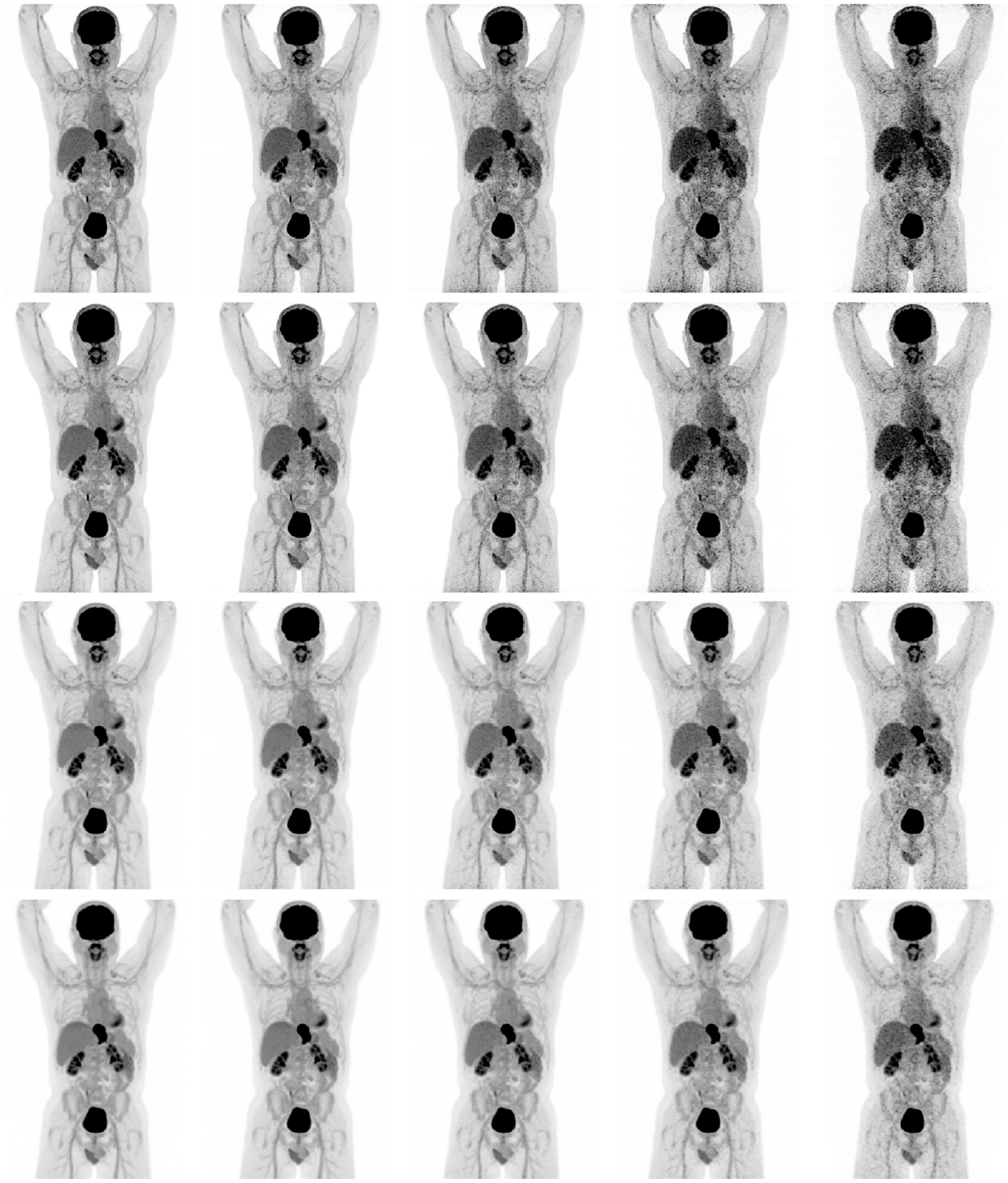

Figure 4 – Maximum intensity projection PET images of a 52-year old male (weight 86 kg) with esophageal cancer acquired at 180, 120, 60, 30, and 10 s/bp (from left to right, respectively) using the Clinical, Clinical+G2, EARL2, and EARL1 reconstruction protocol (from top to bottom, respectively).

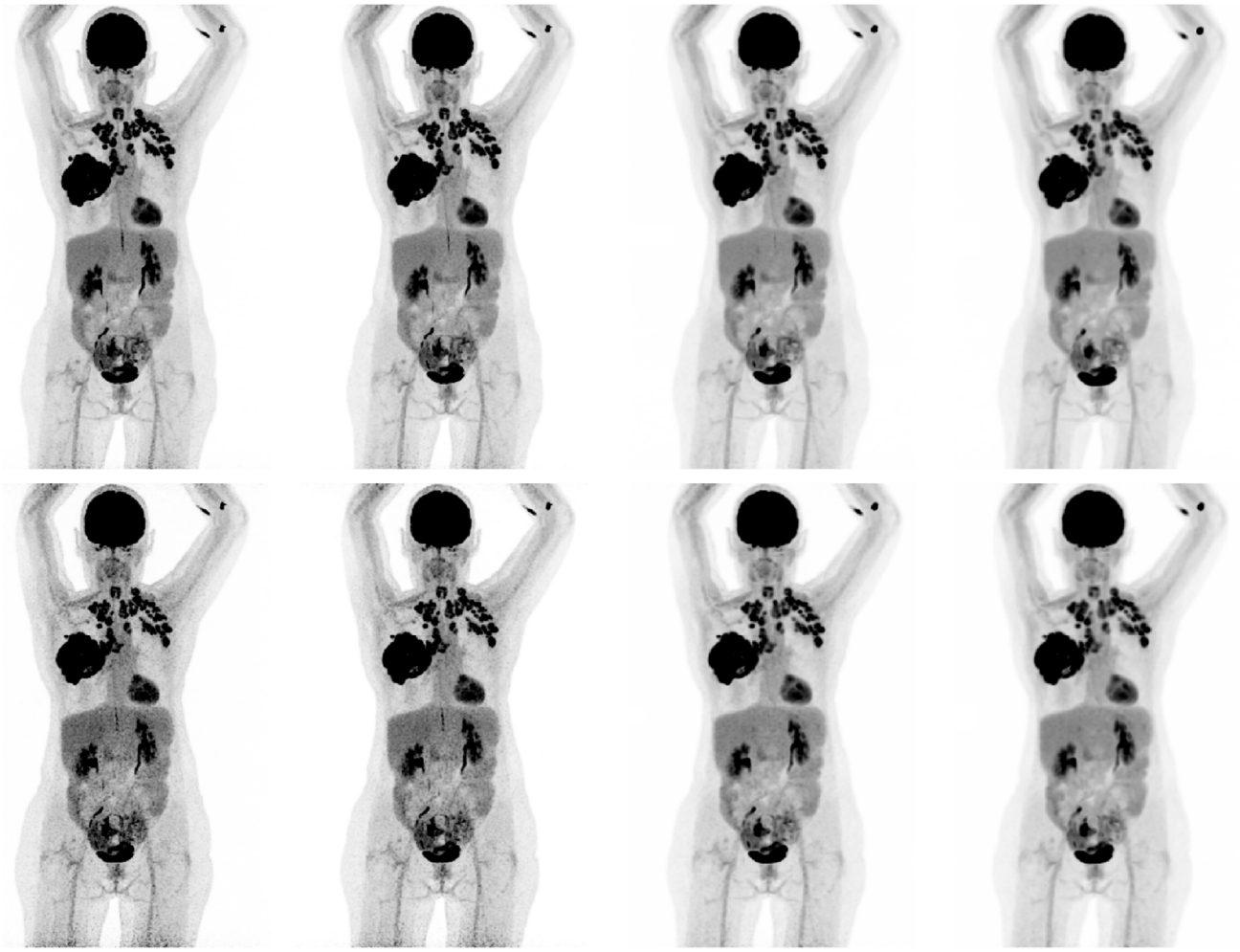

Figure 5 – Maximum intensity projection PET images of a 62-year old female (weight 68 kg) with metastasized NSCLC acquired at 180 s/bp (upper row) and 60 s/bp (lower row) reconstructed using the Clinical, Clinical+G2, EARL2, and EARL1 protocol (from left to right, respectively).

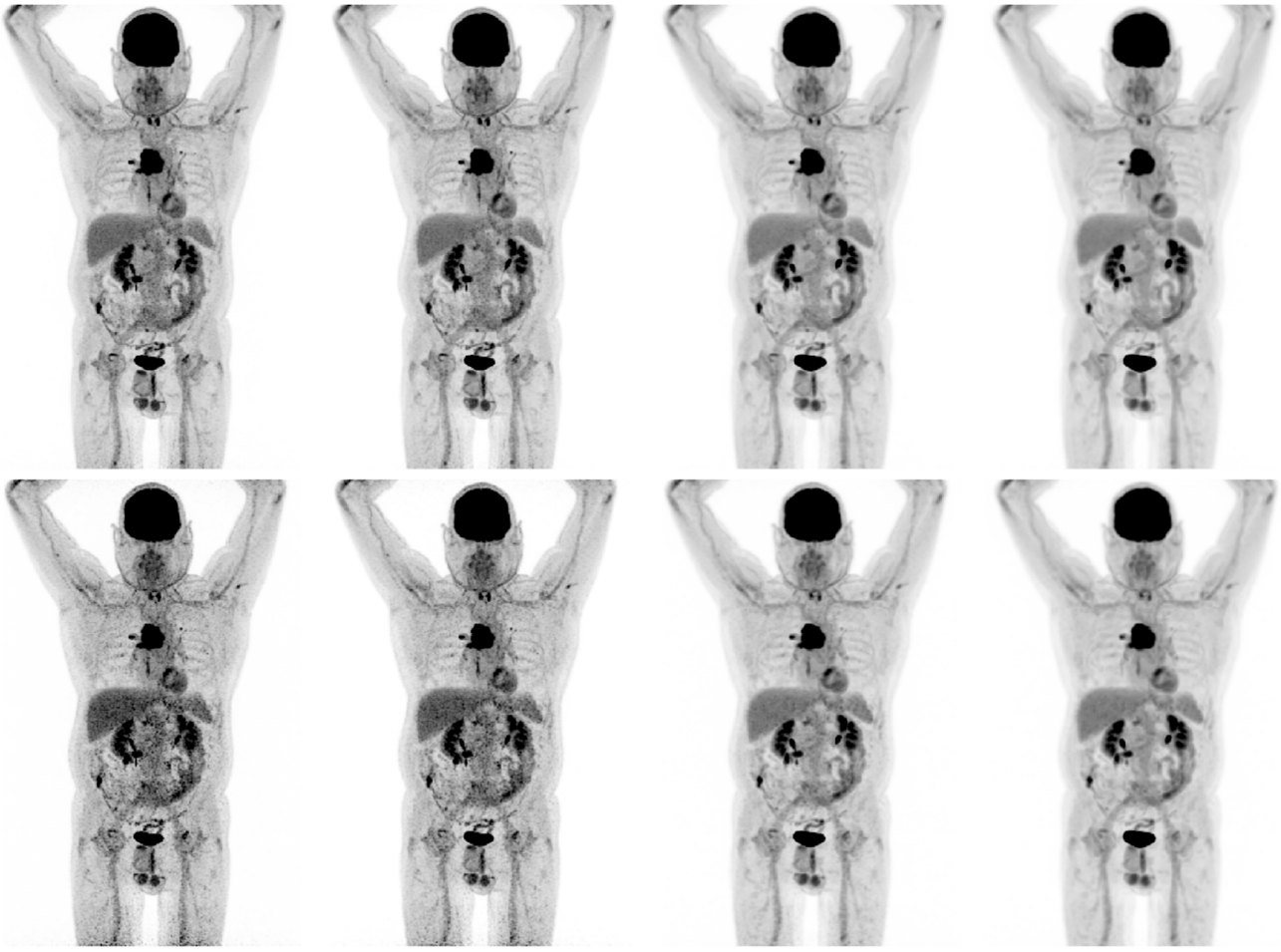

Figure 6 – Maximum intensity projection PET images of a 61-year old male (weight 77 kg) with metastasized NSCLC acquired at 180 s/bp (upper row) and 60 s/bp (lower row) reconstructed using the Clinical, Clinical+G2, EARL2, and EARL1 protocol (from left to right, respectively).

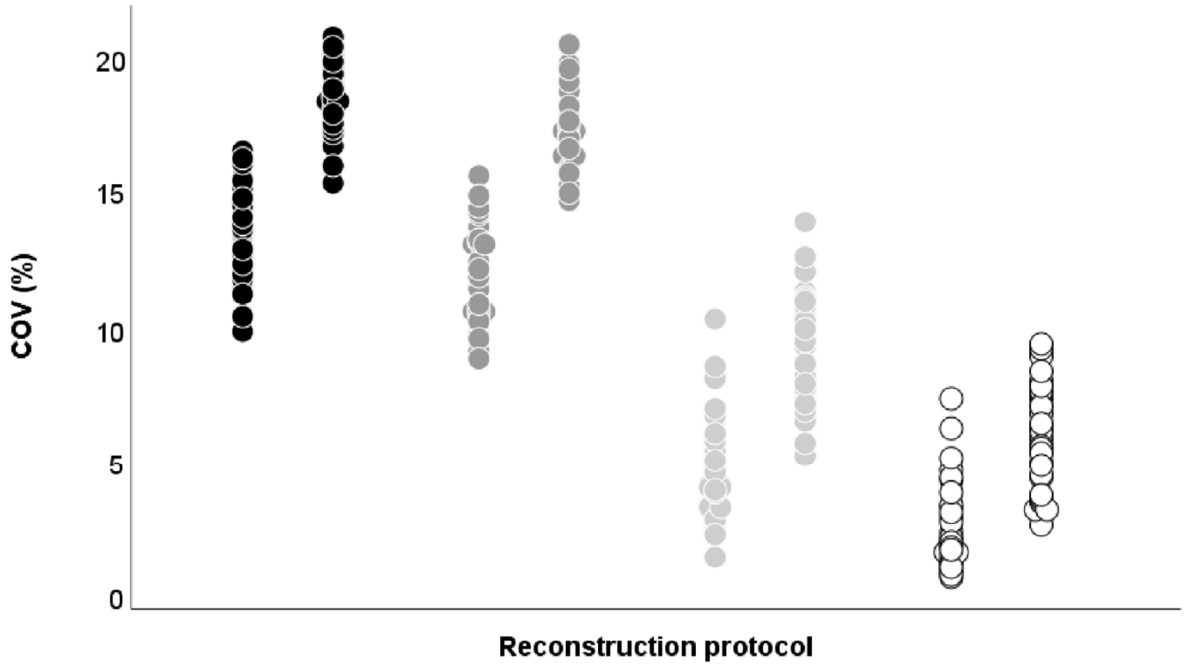

Figure 7 – Liver COV obtained from the Clinical (black), Clinical+G2 (grey), EARL2 compliant (light grey), and EARL1 compliant (white) reconstructed images at 180 s/bp (first column) versus 60 s/bp (second column).

SUPPLEMENTAL

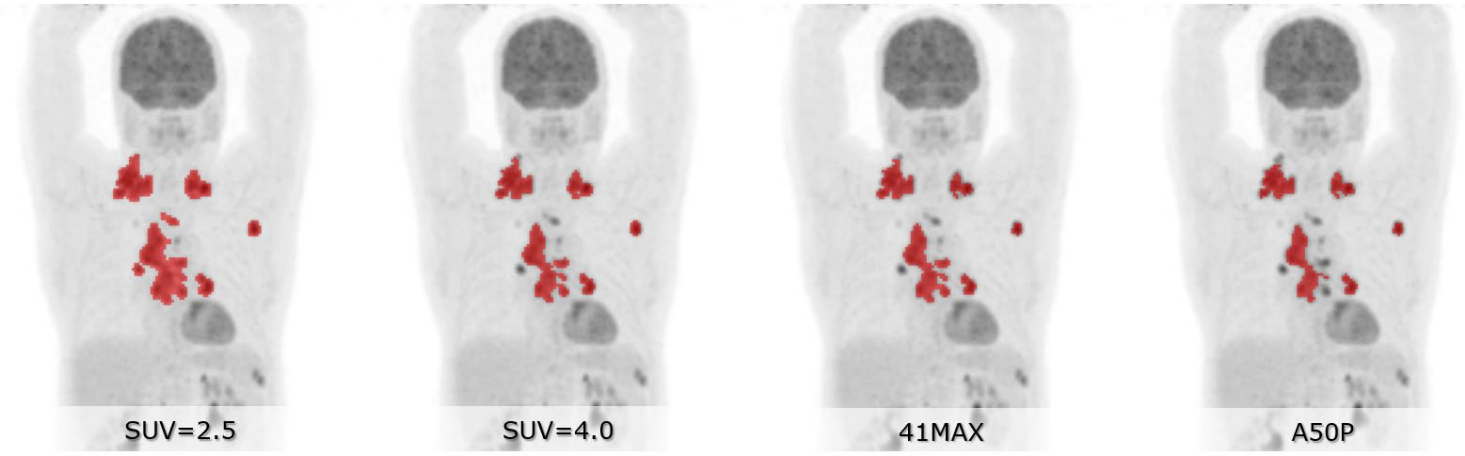

Fixed SUV threshold: 2.5 and 4.0		41% of SUVmax	50% of SUVpeak
231 mL	131 mL	120 mL	95 mL

Supplemental Figure 1 – Clinical example of the segmentation performance of the four standard methods comprising the MV2 delineation method. Clear differences in the segmentation volumes can be observed (in red) for the SUV = 2.5, SUV = 4.0, 41MAX, and A50P method (from left to right).

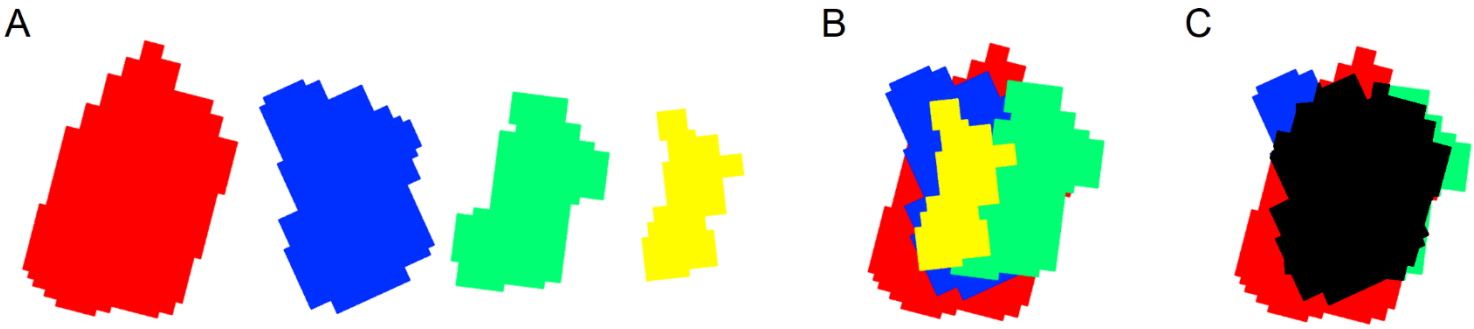

Supplemental Figure 2 – Illustration of the four different segmentation volumes obtained from a single lesion using the four standard segmentation methods comprising the MV2 delineation method: SUV = 2.5 (red), SUV = 4.0 (blue), 41MAX (green), and A50P (yellow) (A). The MV2 method uses the different segmentations of the four methods involved and overlaps the different volumes to evaluate the agreement (B). The resulting MV2 segmentation (black) agrees between at least two of the standard delineation methods.

The Journal of NUCLEAR MEDICINE

Image quality and activity optimization in oncological ^{18}F-FDG PET using the digital Biograph Vision PET/CT

Joyce van Sluis, Ronald Boellaard, Rudi A. Dierckx, Gilles Stormezand, Andor W.J.M. Glaudemans and Walter Noordzij

J Nucl Med.
Published online: October 18, 2019.
Doi: 10.2967/jnumed.119.234351

The Journal of Nuclear Medicine is published monthly.
SNMMI | Society of Nuclear Medicine and Molecular Imaging
1850 Samuel Morse Drive, Reston, VA 20190.
(Print ISSN: 0161-5505, Online ISSN: 2159-662X)

SNMMI SOCIETY OF NUCLEAR MEDICINE AND MOLECULAR IMAGING